Numerical modelling and optimisation of fibre wet-out in resin-injection pultrusion processes

Michael Sandberg[1*], Jesper H. Hattel[1], and Jon Spangenberg[1]

[1]Department of Mechanical Engineering, Section of Manufacturing Engineering,
Technical University of Denmark, Produktionstorvet Building 425, DK-2800 Kgs. Lyngby,
[*]Corresponding author: misan@mek.dtu.dk

Keywords: Resin-injection pultrusion, resin impregnation, level-set method, optimisation, flow-enhancers

Abstract
In this study, a numerical model for the simulation of resin flow in relation to fibre impregnation in resin-injection pultrusion processes has been developed. The model is based on Darcy's law in a 2D finite-volume framework and a level-set method to trace the propagation of the resin flow front. With inspiration from the use of flow-enhancers in other resin transfer moulding processes, the purpose of this study is to explore how local areas with increased permeability can assist in improving the fibre impregnation. Using the numerical model, it is demonstrated how the profile-advancing pulling speed theoretically can be increased by $250-300\%$, while maintaining a complete resin wet-out. This is achieved by increasing the permeability of the profile near the resin inlets, which allows for additional resin flow. Finally, it is demonstrated how an increase in permeability at the centre of the profile can alter the shape of the flow front, which can facilitate complete resin wet-out over a shorter distance.

1 Introduction

Resin injection pultrusion (RIP) is a continuous process for the manufacture of composite profiles with a constant cross-section. In RIP, the fibre material is pulled through an impregnation chamber directly followed by a heating die. In the impregnation chamber, the fibre material is wetted by means of resin injection and in the heating die an exothermic curing reaction is initiated. RIP is a closed mould process, whereby visual inspections and experimental measurements are difficult or impossible to conduct. This means that the implications and sensitivities of different process parameters are often unknown or not fully understood. Numerical simulations are thus important as a tool in the design of new as well as in the optimisation of existing RIP processes.

Among the most important process conditions for composite manufacturing technologies is the resin wet-out of the dry fibre material. Incomplete resin wet-out cannot be accepted as in dry areas of the composite part there exists no adhesion between the matrix (resin) and the fibre material. Following the importance of the impregnation step, the study of resin wet-out in relation to RIP processes has also gained interest in academic research. For example, Sharma et al. [1] studied the pressure build-up in a RIP process using a finite element (FE) numerical simulation framework. In the study, Sharma et al. demonstrated how the pressure build-up in a tapered injection chamber is correlated with the wedge angle for different profile thicknesses. Ding et al. [2] conducted a similar study, but furthermore included the subsequent heat-transfer and curing kinetics in a separate simulation step. Using a finite volume method

(FVM), Palikhel et al. [3] studied the influence of the pulling speed on the fibre wet-out. Palikhel et al. also considered tapering in the injection chamber and its effects on the fibre impregnation. From the same research group, Ranjit et al. [4] investigated the effects of the number of resin inlet slots and their location, and more recently Masuram et al. [5] studied how fibre compaction can influence the fibre wet-out.

As outlined, previous research has been focused on the equipment design, the governing physical phenomena of the resin impregnation, and how these factors play a role in improving the resin wet-out. It has, however, not been studied how local changes in the profile layup can affect the resin flow, which is a common approach for optimisation of the impregnation step in other resin transfer moulding (RTM) processes. Here local, highly permeable layers, such as dedicated flow media or mats, are utilised in the layup to facilitate the resin flow, and it is the goal of this study to explore the effects of using these options in RIP processes.

In the present study, the impregnation stage in a RIP process is considered. An impregnation model that follows Darcy's law for flow in anisotropic porous media is developed, with an advective term in order to account for the pulling speed. The fibre impregnation is simulated in a 2D FVM based numerical framework, with a level-set free-surface modelling technique to trace the propagation of the resin flow front. Using the numerical model, the process optimisation and parameter study follow a criterion of maximising pulling speed (production output), while maintaining complete resin wet-out at a constant injection pressure.

2 Methods

2.1 Flow model

In this study, the flow is considered to be saturated, creeping and incompressible. Consequently, Darcy's law [6] can be used to describe the relationship between the spatial velocities and the pressure gradient

$$u_i = -\frac{k_{ij}}{\mu\theta^p} p_{,j} + U_i^a = -K_{ij} p_{,j} + U_i^a \tag{1}$$

where k_{ij} is the permeability tensor, μ is the dynamic viscosity, u_i are the spatial velocities of the fluid with respect to the coordinate x_i, θ^p is the porosity of the dry fibre media (fraction of initial void space), and $p_{,i}$ is the pressure gradient. Finally, U_i^a is the constant advection to account for the pulling speed, and for brevity the Darcy coefficient $K_{ij} = k_{ij}/(\mu\theta^p)$ is defined. Throughout this paper, Einstein's summation rule applies to tensor equations, and $(\,)_{,i}$ denotes partial differentiation.

Eq. (1) must obey mass conservation, $u_{i,i} = 0$, meaning

$$(K_{ij} p_{,j})_{,i} = 0 \tag{2}$$

which constitutes the relation between velocity and pressure. Please note that U_i^a is omitted from the conservation equation as it is constant everywhere in the domain.

2.2 Free-surface modelling technique

During the impregnation step, the resin flow front advances and the fluid domain expands. For tracking the development of the flow front, the level-set method is applied [7]. In this approach, the level set equation holds the absolute distance to the interface. Thereby, it is a signed distance function, which has a Euclidean norm of unity ($||\phi_{,i}|| = 1$) everywhere in the domain. The wet domain, Ω_{wet}, the dry domain,

Ω_{wet}, and the fluid interface, $\Gamma_{interface}$, are then defined by the level-set as

$$\begin{cases} \phi(x,t) < 0 & \text{in} \quad \Omega_{wet} \\ \phi(x,t) = 0 & \text{on} \quad \Gamma_{interface} \\ \phi(x,t) > 0 & \text{in} \quad \Omega_{dry} \end{cases} \tag{3}$$

The level set equation follows the advection equation

$$\phi_{,t} + u_i \phi_{,i} = 0 \tag{4}$$

where $(\,)_{,t}$ is the time derivative. The spatial velocities, u_i, are determined from Eq. (1).

After evolving the level-set equation through advection in the velocity field, ϕ does generally not maintain the property of being a signed distance function ($||\phi_{,i}|| \neq 1$) . For this reason, one needs to reinitialise the level-set by solving the following equation to steady state [7]

$$\phi_{,t} = S_\varepsilon(\phi)(1 - ||\phi_{,i}||) \tag{5}$$

where $S_\varepsilon(\phi)$ is a smeared-out sign function.

2.3 Numerical discretisation

The spatial discretisation of the governing equations for the fluid flow is obtained using FVM on a staggered grid structure. In this framework, the pressure from Eq. (2) lies in the cell centres, whereas the spatial velocities (Eq. 1) lie on the cell faces. The scheme for the pressure is established by considering conservation of mass on a cell-volume basis and applying Gauss's theorem

$$\int_\Omega \left(\frac{k_{ij}}{\mu \theta^p} p_{,j} \right)_{,i} \mathrm{d}\Omega = \int_S \frac{k_{ij}}{\mu \theta^p} p_{,j} n_i \mathrm{d}S \tag{6}$$

The viscosity is dependent on whether the cell is occupied by air or resin. This is implemented through the Darcy coefficient, which follows the function

$$K_{ij}(\phi) = K_{ij}^a + (K_{ij}^r - K_{ij}^a) \frac{1}{1 + \exp(-\phi/\gamma)} \tag{7}$$

where the smoothing parameter, γ, is set to $\gamma = 1/5 \cdot \max(\Delta x, \Delta y)$. The cell-face value of the Darcy coefficient is determined by the harmonic mean of the two adjacent cells. A viscosity ratio between the resin and air of $\mu^a = 10^{-6}\mu^r$ is used in calculations.

The same discretisation method is applied for the advection of the level-set equation (Eq. 4) and the reinitialisation thereof (Eq. 5). The values of ϕ lie in the cell centres and the face values of ϕ are estimated using a 5th-order weighted essentially non-oscillatory (WENO) scheme, with upwinding through the Godunov method [8]. Finally, the level-set equation is only advected and reinitialised in a narrow band of $6 \cdot \max(\Delta x, \Delta y)$ in accordance with [9]. The temporal discretisation follows a 3rd-order Runge-Kutta method.

2.4 Domain, boundary conditions, material properties and estimates of permeabilities

To summarise, the solution of the governing equations involves: i) solving for the pressure in the cell centres (Eq. 2); ii) calculation of the velocities on the cell faces (Eq. 1); and finally iii) advection and reinitialisation of the level-set equation (Eqs. 4-5). This is conducted using the technical programming language Matlab™.

The domain and boundary conditions are shown in Fig. 1. The numerical model represents the resin wet-out of a thick composite profile in a straight impregnation chamber with overall dimensions of $L_{x_1} \times L_{x_2} = 0.5\text{ m} \times 0.08\text{ m}$. This follows the example presented in [10]. The pulling speed in the x_1-direction is constant with a speed of U_1^a (specified in subsequent sections), and zero in the x_2-direction. The resin is injected at an injection pressure of $p_{\text{inj}} = 20$ bar (w.r.t. atmospheric pressure) through an injection slot of 0.03 m, which is imposed through a Dirichlet boundary condition. Similarly, at the left side of the domain, that is the entrance of the impregnation chamber, atmospheric pressure ($p = p_{\text{atm}} = 0$) is imposed. Neumann boundary conditions are imposed at the top and bottom parts of the profile, which implies that the pressure gradient in the x_2-direction, $p_{,2}$, vanishes at the horizontal mould surfaces. Finally, the pressure gradient at the exit of the impregnation chamber is set to zero ($p_{,1}$), meaning the resin velocity attains the advection speed of the profile, U_1^a, at the exit of the chamber. Symmetry is exploited at the centreline of the domain, and this part is decomposed into a structured Cartesian grid of 100×20 cells.

The resin is a thermoset polyester resin with a viscosity of $\mu = 0.2$ Pa·s. The fibre volume fraction is $\theta^f = 0.45$ [-] and the fibre porosity follows the relation $\theta^p = 1 - \theta^f$. The fibre radius is $R = 17/2\ \mu$m. To give estimates of magnitudes of permeabilities in the fibre material, the measures from Gebert [11] are used:

$$k_{11} \approx 8R^2 \frac{1}{a} \frac{(1-\theta^f)^3}{(\theta^f)^2}, \quad k_{22} \approx bR^2 \left(\sqrt{\theta^{f,max}/\theta^f} - 1 \right)^{5/2} \tag{8}$$

where the remaining constants are chosen according to [11]: $a = 53$ (hexagonal stacking), $b = 16/(9\pi\sqrt{6})$, $\theta^{f,max} = \pi/(2\sqrt{3})$. Off-diagonal terms in the permeability tensor, k_{ij}, are set to zero. From Eq. (8), the following permeabilities are estimated: $k_{11} = 8.98 \cdot 10^{-12}$ m^2 (along the fibres), $k_{22} = 1.90 \cdot 10^{-12}$ m^2 (perpendicular to the fibres).

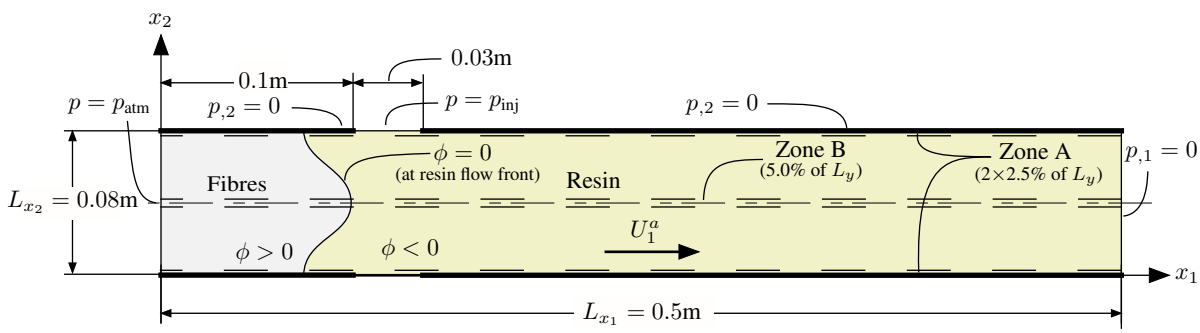

Figure 1: Numerical model with boundary conditions.

3 Results and discussion

As the scope of this paper is to study how areas with increased permeability can facilitate improved resin flow, it is briefly discussed at what level local changes in permeability are physically justifiable in a realistic pultrusion process.

To a large extent, a desired local variance in permeability can be achieved by the choice of roving type. A rough estimate based on Eq. (8) shows that the permeability scales proportionally to R^2, which means that if the radius of the fibre type is doubled, the permeability increases fourfold. Variances in permeability are also highly dependent on the local volume fraction, which will be dependent on the fibre architecture of the roving type. Naturally, a roving type with a loose fibre-architecture, such as multi-end, mock or spun rovings, will have a lower volume fraction compared to single-end, direct rovings. If, for example, estimates are based on Eq. (8), the permeability of rovings will increase by more than a factor of seven if the fibre volume fraction is lowered from $v_f = 0.6$ to $v_f = 0.4$[-]. Another approach is to include chopped

strand mats (CSM), continuous filament mats (CFM), or other high-porosity fibre reinforcements in the profile layup. According to [12, 13] a permeability in the order of 10^{-9} to 10^{-10}[m^2] for CSM and CFM reinforcements can be expected, which is up to a thousandfold increase in permeability when compared to the estimates for rovings provided in Section 2.4.

As outlined in this section, conventional fibre materials employ a rather wide variety of permeabilities. In this study, however, only a narrow range of this design freedom will be exploited, as only a tenfold increase in local permeability will be considered.

3.1 Case A: Increased permeability in the upper and lower part of the profile

The basis for the parameter study in Case A is the local permeability in the upper and lower 2.5% of the profile thickness (c.f. Fig. 1). In these areas, the permeability is increased to a factor of $K_a = 10.0$ in increments of 2.5. The permeability in both directions is considered to scale linearly. The pulling speed is set to $U_1^a = 0.35$m/min. The stationary flow front positions can be seen in Fig. 2 and the stationary pressure field in Fig. 3 for a selected number of cases.

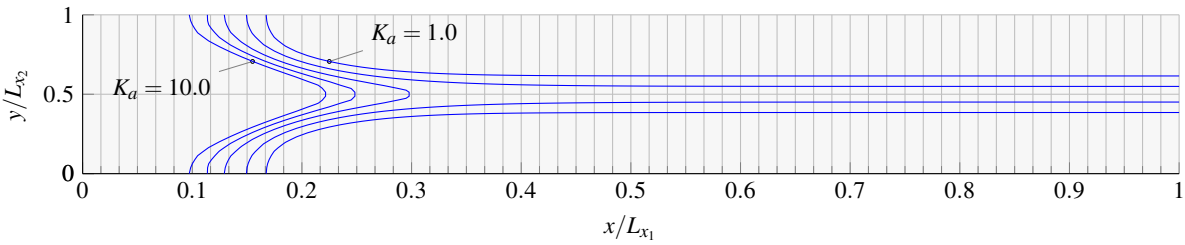

Figure 2: Stationary flow front positions for $K_a = 1.0, 2.5, 5.0, 7.5, 10.0$, $K_b = 1$ (see Fig. 1) and constant pulling speed of $U_1^a = 0.35$m/min.

As it can be seen in Fig. 2, the profile with homogeneous permeability ($K_a = 1.0$) does not achieve complete wet-out at the exit of the impregnation chamber. Increasing the permeability in Zone A, however, significantly improves the resin wet-out. With $K_a = 5.0$, the full cross-section of the profile achieves complete wet-out, and with even higher permeability ($K_a = 10.0$), the flow front moves further back and an increase in pressure build-up is obtained.

Fig. 3 demonstrates that a complete resin wet-out of the profile leads to a pressure build-up at the exit of the impregnation chamber. A build-up of pressure can also be considered positive, as it will aid in the saturation of any local fibre-rich areas. Therefore, a robust criterion for achieving a complete resin wet-out must consider this pressure build-up. To exemplify a possible enhancement in pulling speed, two thresholds for complete wet-out are selected. These limits are based on the fraction of the inlet pressure that is maintained at the exit of the impregnation chamber and are set to, respectively, 20% and 50% of the inlet pressure, p_{inj}. The achievable pulling speed for the cases considered can be seen in Fig. 4. As the figure shows, a notable improvement is obtained. From the reference configuration with $K_a = 1$, the pulling speed can be increased by 250% ($p_{\text{limit}} = 50\% p_{\text{inj}}$) to 300% ($p_{\text{limit}} = 20\% p_{\text{inj}}$) when the increase of permeability in Zone A is set to $K_a = 10$.

Clearly, by introducing a highly permeable layer near the inlets, the resin wet-out is improved. This physical correlation is also reasonable to expect, as a highly permeable area near the inlet will increase the mass flux of resin into the domain. The additional resin flowing into the profile simply translates into a larger amount of fibres being impregnated, and this allows for, as demonstrated, an increase in pulling speed.

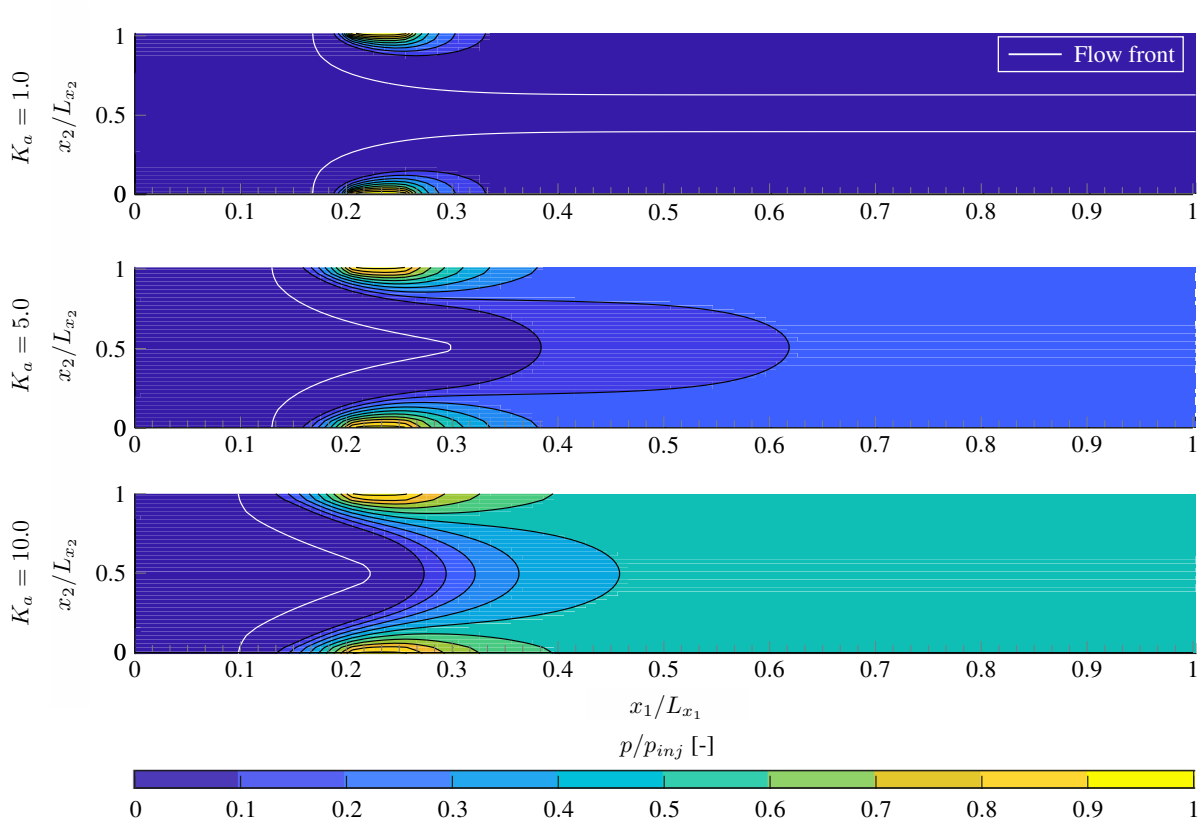

Figure 3: Stationary pressure field with flow front positions for $K_a = 1.0, 5.0, 10.0$, $K_b = 1$ (see Fig. 1) and constant pulling speed of $U_1^a = 0.35$m/min

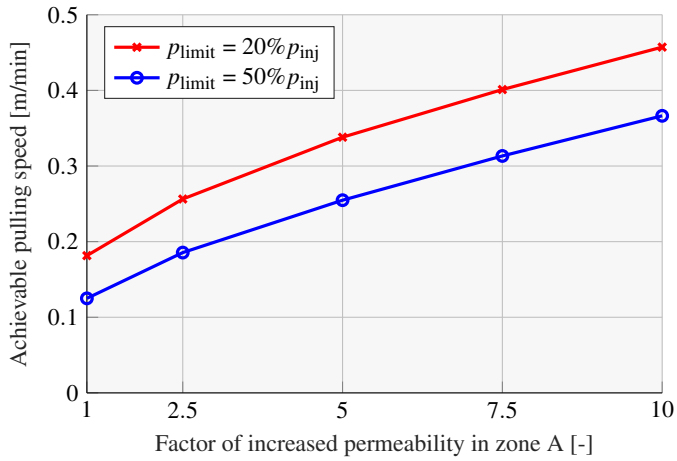

Figure 4: Achievable pulling speed for $K_a = 1.0, 2.5, 5.0, 7.5, 10.0$, $K_b = 1$ (see Fig. 1). p_{limit} is the threshold for pressure build-up at the exit of the impregnation chamber.

3.2 Case B: Increased permeability in the centre of the profile

The final example concerns the effect of increasing the permeability in the centre of the profile. Here, the permeability in the middle 5% of the profile height, L_{x_2}, is increased by a factor of $K_b = 10.0$ in increments of 2.5, which is identical to the procedure in Case A. As an increase in the permeability in the centre of the profile does not facility any resin flow if the flow front never reaches this region, the pulling speed is lowered to $U_1^a = 0.12$m/min. This is to achieve a complete resin wet-out and a pressure

build-up of approximately 50% of the injection at the exit of the impregnation chamber. The stationary flow front positions are presented in Fig. 5. It is seen that an increase in permeability in the centre of the profile can be used to alter the shape of the flow front. This local permeability introduces a back-flow in the centre of the profile, which facilitates complete resin wet-out over a shorter distance.

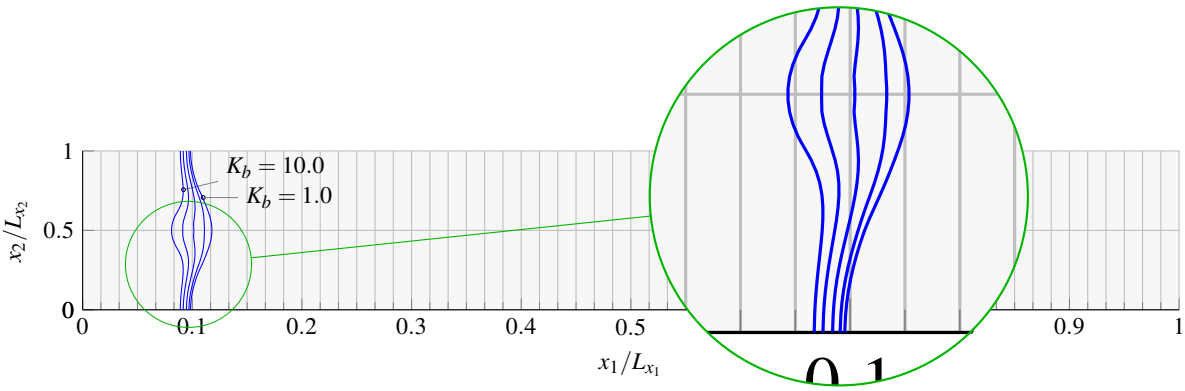

Figure 5: Stationary flow front positions for $K_b = 1.0, 2.5, 5.0, 7.5, 10.0$, $K_a = 1$ (see Fig. 1) and constant pulling speed of $U_1^a = 0.12$m/min.

4 Conclusions

The results presented in this paper demonstrate the possible benefits of including local areas with increased permeability in the design of the profile layup in resin-injection pultrusion processes. This design approach is similar to the use of flow enhancers in other resin transfer moulding processes.

Two different scenarios were studied in this paper. The first example considered increasing the permeability of a factor of 10 at the upper and lower 2.5% of the profile. This corresponds to the regions of the profile closest to the resin inlets, and it was demonstrated that the pulling speed can theoretically be increased by $250-300\%$ while maintaining a complete resin wet-out. Finally, it was studied how the same level of modification affects the resin flow when the permeability in the centre of the profile is changed. For this case, it was demonstrated that a local back-flow in the centre of the profile is obtained, and this allows for complete resin wet-out over a shorter distance.

In future research, we aim to expand the numerical framework into 3D and explore more complex variances in permeability in combinations with different resin-injection strategies.

Acknowledgments

This work is funded by the Danish Council for Independent Research — Technology and Production Sciences (Grant no. DFF-6111-00112: Modelling the multi-physics in resin injection pultrusion (RIP) of complex industrial profiles).

References

[1] D Sharma, T A Mccarty, J A Roux, and G Vaughan. Fluid mechanics analysis of a two-dimensional pultrusion die inlet. *Polymer Engineering & Science*, 38(10):1611–1622, 1998.

[2] Zhongman Ding, Shoujie Li, Huan Yang, L. James Lee, Herbert Engelen, and P. M. Puckett. Numerical and experimental analysis of resin flow and cure in resin injection pultrusion (RIP). *Polymer Composites*, 21(5):762–778, 2000.

[3] D. R. Palikhel, J. A. Roux, and A. L. Jeswani. Die-attached versus die-detached resin injection chamber for pultrusion. *Applied Composite Materials*, 20(1):55–72, 2013.

[4] S Ranjit, J A Roux, and A L Jeswani. Impact of Single and Multiple Injection Slot Locations for Attached- Die and Detached-Die Tapered Resin Injection Pultrusion. *Polymers & Polymer Composites*, 22(6):495–508, 2014.

[5] N B Masuram, J A Roux, and A L Jeswani. Pull Speed Influence on Fiber Compaction and Wetout in Tapered Resin Injection Pultrusion Manufacturing. *Polymers & Polymer Composites*, 25(6):419–434, 2017.

[6] Henry Darcy. Les fontaines publiques de la ville de Dijon. *Victor Dalmont, Libraire des Corps imperiaux des ponts et chaussées et des mines*, 1856.

[7] Mark Sussman, Peter Smereka, and Stanley Osher. A Level Set Approach for Computing Solutions to Incompressible Two-Phase Flow. *Journal of Computational Physics*, 114(1):146–159, 1994.

[8] Chi-Wang Shu. High Order Weighted Essentially Nonoscillatory Schemes for Convection Dominated Problems. *SIAM Review*, 51(1):82–126, 2009.

[9] Danping Peng, Barry Merriman, Stanley Osher, Hongkai Zhao, and Myungjoo Kang. A PDE-Based Fast Local Level Set Method. *Journal of Computational Physics*, 155(2):410–438, 1999.

[10] Jon Spangenberg, Martin Larsen, Rosa R Rodríguez, Pablo M M Sánchez, Filip S Rasmussen, Mads R Sonne, and Jesper H Hattel. The effect of saturation on resin flow in injection pultrusion: A preliminary numerical study. In *21st International Conference on Composite Materials (ICCM-21)*, Xi'an, 2017.

[11] B. R. Gebart. Permeability of Unidirectional Reinforcements for RTM. *Journal of Composite Materials*, 26(8):1100–1133, 1992.

[12] M S Koefoed. *Modeling and Simulation of the VARTM Process for Wind Turbine Blades*. Phd thesis, Aalborg University, 2003.

[13] R Bezerra, F Wilhelm, and F Henning. Compressibility and Permeability of Fiber Reinforcements for Pultrusion. In *16th European Conference on Composite Materials*, 2014.